

Static and Dynamic Swelling of Grafted Poly(2-alkyl-2-oxazoline)s

Florian Rehfeldt and Motomu Tanaka*

Lehrstuhl für Biophysik, Technische Universität München, James-Franck-Strasse, 85748 Garching, Germany

Lorena Pagnoni and Rainer Jordan*

Lehrstuhl für Makromolekulare Stoffe, Technische Universität München, Lichtenbergstrasse 4, 85747 Garching, Germany

Received August 7, 2001. In Final Form: March 18, 2002

Poly(2-methyl-2-oxazoline) (PMOX) and poly(2-ethyl-2-oxazoline) (PEOX) bearing trimethoxysilane end groups for surface coupling were synthesized and grafted onto silicon/silicon dioxide substrates. Static and dynamic hydration of these films by water vapor was quantitatively studied by ellipsometry. The static swelling behavior was analyzed by measuring the equilibrium film thickness as a function of the relative humidity to obtain quantitative force–distance curves. The disjoining pressure measures the sum of all operating forces in equilibrium with the chemical potential of the surrounding atmosphere, where the dominant forces could be determined. The hydration of polymers with different initial thickness was compared by the normalized swelling ratio ρ and the calculated decay constant λ^* . All the measured parameters exhibited a clear dependence upon the chain length. The dynamic swelling behavior was studied by monitoring the film thickness as a function of time under an “osmotic shock”, switching from dry to humid atmospheric conditions (relative humidity from ~4% to ~90%). The characteristic time constants were analyzed for each derivative semiquantitatively, indicating that the kinetics of the water uptake is dependent on the polymer length rather than on the side chains.

Introduction

The design of functional soft interface layers between solid semiconductor surfaces and biological systems such as proteins and cells includes numerous scientific and practical applications.¹ One of the possible strategies to fabricate such biocompatible surfaces is the deposition (e.g., grafting, casting, spin-coating, and layer-by-layer transfer) of thin ($d < 100$ nm) hydrated polymer films on the surface. Practically, this strategy can be applied for proliferation and stress-free immobilization of cells, enzymes, and receptors under non-denatured conditions to utilize their native functions for sensor application or alarm systems with intrinsic amplification. Scientific aspects include the creation of model extracellular matrices (ECMs) to control cell–cell and cell–tissue interactions by the chemical nature and morphology of polymers.

Cell surface glycocalyx and ECMs in nature maintain high local disjoining pressures and control the “wetting affinity” between cells and tissues by the combination of weak, generic forces at interfaces.^{1,2} For example, at repulsive disjoining pressures, a cell can keep a certain distance from other cells and proteins via hydrated “cushions”. However, strong nonspecific adsorption can take place when the interfacial interaction becomes attractive.³ Indeed, recent studies have demonstrated that the phase separation induced by strong adhesion can even be interpreted as the first-order wetting/dewetting transition.⁴ To design better-defined physical models of ECMs

and glycocalyx based on synthetic polymers, quantitative studies on their interaction with the water, e.g., wetting properties and kinetic of water uptake, are prerequisite. To date, a sufficient biocompatibility that prevents nonspecific adsorption of proteins and cells could be achieved by grafted films of dextran⁵ and poly(ethylene glycol) (PEG) derivatives,⁶ which have been used in numerous fields. When the films of functionalized PEG derivatives are covalently end-grafted, the protein/cell resistance of the films can be interpreted in terms of phenomenological steric repulsion forces^{7–10} and, therefore, strongly depend on the chain length,¹¹ grafting density,^{12,13} surface coupling groups,^{14–16} and morphology of chains.^{17,18}

In contrast to the commonly used PEG systems, poly-(2-alkyl-2-oxazoline)s, synthesized by living cationic

* To whom correspondence may be addressed: Motomu Tanaka, tel ++49-89-289-12539, fax ++49-89-28912469, e-mail mstanaka@ph.tum.de; Rainer Jordan, tel ++49-89-289-13581, fax ++49-89-28913562, e-mail rainer.jordan@ch.tum.de.

(1) Sackmann, E.; Tanaka, M. *Trends Biotechnol.* **2000**, *18*, 58.
(2) Comper, W. D. *Extracellular Matrix*; Harwood Academic Publishers: Amsterdam, 1996.
(3) Elender, G.; Sackmann, E. *J. Phys. II* **1994**, *4*, 455.

(4) Bruinsma, R.; Behrisch, A.; Sackmann, E. *Phys. Rev. E* **2000**, *61*, 4253.
(5) Löfas, S.; Johnson, B. *J. Chem. Soc., Chem. Commun.* **1990**, *21*, 1526.
(6) Andrade, J. D.; Hlady, V. *Adv. Polym. Sci.* **1986**, *79*, 1.
(7) Taunto, H. J.; Toprakcioglu, C.; Fetters, L. J.; Klein, J. *Nature* **1988**, *332*, 712.
(8) Jeon, S. I.; Andrade, J. D. *J. Colloid Interface Sci.* **1991**, *142*, 159.
(9) Jeon, S. I.; Lee, J. H.; Andrade, J. D.; de Gennes, P. D. *J. Colloid Interface Sci.* **1991**, *142*, 149.
(10) Halperin, A. *Langmuir* **1999**, *15*, 2525.
(11) Yang, Z.; Galloway, J. A.; Yu, H. *Langmuir* **1999**, *15*, 8405.
(12) Schröen, C. G. P. H.; Cohen Stuart, M. A.; Voort Maarchalk van der, K.; Padt van der, A.; Riet van't, K. *Langmuir* **1995**, *11*, 3068.
(13) Sofia, S. J.; Premnath, V.; Merrill, E. W. *Macromolecules* **1998**, *31*, 5059.
(14) Herren, B. J.; Shafer, S. G.; Alstine van, J.; Harris, J. M.; Snyder, R. T. *J. Colloid Interface Sci.* **1987**, *115*, 46.
(15) Kiss, E.; Gölander, C. G. *Colloids Surf.* **1990**, *49*, 335.
(16) Burns, N. L.; Alstine van, J. M.; Harris, J. M. *Langmuir* **1995**, *11*, 2768.
(17) Nashabeh, W.; El Rassi, Z. *J. Chromatogr.* **1991**, *559*, 367.
(18) Elbert, D. L.; Hubbell, J. A. *Annu. Rev. Mater. Sci.* **1996**, *26*, 365.

polymerization, provide the possibility to tailor macromolecules by the choice of different side substitutions and terminal groups.^{19–22} Since the length of the alkyl chain in the 2-position determines the hydrophilicity of each monomer unit,^{23,24} polymers of 2-methyl- and 2-ethyl-2-oxazolines are potential candidates to form hydrophilic polymer films.^{25,26} The biocompatibility and interface characteristics of these poly(2-oxazoline) derivatives were investigated elsewhere.^{27–31} For example, lipid vesicles doped with poly(2-oxazoline) lipopolymers showed remarkably larger blood circulation times than ordinary phospholipid vesicles,²⁸ which are even comparable to conventional PEG lipopolymers. However, quantitative investigations on their interaction with water are still missing.

Previously, we reported the modification of gold substrates by the surface-initiated polymerization of hydrophilic poly(2-ethyl-2-oxazoline),^{32,33} using self-assembled monolayers as initiating sites. Although the grafting density obtained by this “grafting from” technique is higher than that prepared by the “grafting onto” method, the specification of the film is difficult because of the unknown degree of polymerization and polydispersity index (PDI). Hence, in this study, three types of poly(2-alkyl-2-oxazoline)s with a terminal trimethoxysilane group were synthesized by cationic living polymerization and grafted onto silicon/silicon dioxide surfaces.^{20,22,34}

To investigate static and dynamic swelling behaviors of grafted poly(2-alkyl-2-oxazoline) brushes, the film thickness was measured quantitatively by ellipsometry coupled to a climate chamber. Ellipsometry is a noninvasive, powerful technique with a high thickness resolution (± 0.1 Å) to study such soft, hydrated polymer films.^{3,35,36} The static swelling behavior was studied by measuring the equilibrium film thickness as a function of the relative humidity to obtain force–distance curves, i.e., disjoining pressure plotted as a function of film thickness. The dynamic swelling behavior was studied by monitoring the change of the film thickness as a function of time after an “osmotic shock” (i.e., abrupt change of the relative humidity) in order to investigate the kinetics of the hydration. Effects of polymer chain length ($n = 15$ and 30 , $PDI = 1.09–1.24$) and side chains (CH_3- and C_2H_5-) are systematically discussed in the following sections.

- (19) Kobayashi, S.; Iijima, S.; Igarashi, T.; Saegusa, T. *Macromolecules* **1987**, *20*, 1729.
 (20) Jordan, J.; Graf, K.; Riegler, H.; Unger, K. K. *Chem. Commun.* **1996**, *9*, 1024.
 (21) Lehmann, T.; Rühle, J. *Macromol. Symp.* **1999**, *142*, 1.
 (22) Jordan, R.; Martin, K.; Räder, H.-J.; Unger, K. K. *Macromolecules* **2001**, *34*, 8858.
 (23) Bassiri, T. G.; Levy, A.; Litt, M. *J. Polym. Sci. B* **1969**, *7*, 463.
 (24) Litt, M.; Rahl, F.; Roldan, L. G. *J. Polym. Sci. A-2* **1969**, *7*, 463.
 (25) Kobayashi, S. *Prog. Polym. Sci.* **1990**, *15*, 751.
 (26) Aoi, K.; Okada, M. *Prog. Polym. Sci.* **1996**, *21*, 151.
 (27) Velander, W. H.; Madurawe, R. D.; Subramanian, A.; Kumar, G.; Sinai-Zingde, G.; Riffle, J. S. *Biotechnol. Bioeng.* **1992**, *39*, 1024.
 (28) Woodle, M. C.; Engbers, C. M.; Zalipsky, S. *Bioconjugate Chem.* **1994**, *5*, 493.
 (29) Lasic, D. D.; Needham, D. *Chem. Rev.* **1995**, *95*, 2601.
 (30) Bækmark, T. R.; Wiesenthal, T.; Kuhn, P.; Bayerl, T. M.; Nuyken, O.; Merkel, R. *Langmuir* **1997**, *13*, 5521.
 (31) Wurlitzer, A.; Politsch, E.; Huebner, S.; Krüger, P.; Weygand, M.; Kjaer, K.; Hommes, P.; Nuyken, O.; Cevc, G.; Lösche, M. *Macromolecules* **2001**, *34*, 1334.
 (32) Jordan, R.; Ulman, A. *J. Am. Chem. Soc.* **1998**, *120*, 243.
 (33) Jordan, R.; West, N.; Ulman, A.; Chou, Y.-M.; Nuyken, O. *Macromolecules* **2001**, *34*, 1606.
 (34) Chujo, Y.; Ihara, E.; Ihara, H.; Saegusa, T. *Macromolecules* **1989**, *22*, 2040.
 (35) Elender, G.; Kühner, M.; Sackmann, E. *Biosens. Bioelectron.* **1996**, *11*, 565.
 (36) Mathe, G.; Albersdörfer, A.; Neumaier, K. R.; Sackmann, E. *Langmuir* **1999**, *15*, 8726.

Experimental Section

Synthesis of Silane-Functionalized Poly(2-oxazoline)s.

All polymerizations were carried out in a Schlenk tube under inert nitrogen atmosphere using freshly distilled and dried solvents. Details of the preparation such as purification of solvents and the 2-oxazoline monomers were reported previously.^{22,32,37} Solvents and conditions for the final silane-functionalized polymers were made under anhydrous conditions to avoid hydrolysis and condensation of the trimethoxysilane groups. A 0.3 mol (0.15 mol for $DP = 15$) quantity of 2-ethyl- or 2-methyl-2-oxazoline (Aldrich) was added to a prepared solution of 0.01 mol of methyl trifluoromethanesulfonate (Aldrich) in 40 mL of acetonitrile at 0 °C. The reaction mixture was then refluxed for at least 24 h.

For the terminal functionalization of the polymer, the reaction mixture was cooled to 0 °C, and 0.025 mol of 3-aminopropyltrimethoxysilane (ABCR, Karlsruhe, Germany) was added. Then the temperature was elevated to room temperature and the mixture was allowed to react for another 24 h. After removal of the solvent, the residue was dissolved in 10 mL of dry CH_2Cl_2 and 2 g of finely ground K_2CO_3 (Merck, Darmstadt, Germany) was added. After the mixture was stirred overnight, the suspension was filtered (PTFE filter $\phi = 0.45$ μm ; Satorius) and the clear solution was transferred into 200 mL of dry and degassed diethyl ether to precipitate a white powder. After two reprecipitation cycles ($\text{CHCl}_3/\text{diethyl ether}$), the final product was collected and freeze-dried using dry benzene, yielding a hygroscopic colorless powder.

¹H NMR (300 MHz) spectra were recorded in CDCl_3 using an ARX 300 (Bruker, Karlsruhe, Germany), and FTIR spectra were measured by IFS 55 (Bruker) accumulating 32 scans of a thin drop-casted polymer film (KBr window, transmission mode) at 2 cm^{-1} spectral resolution for each spectrum. Gel permeation chromatography (GPC) was carried out on a GPC 510 (Waters), using polystyrene standards for calibration.

Substrates. p-type boron doped silicon [100] wafers (Wacker Siltronic, Burghausen, Germany) with specific resistance of $R = 4.5–6.0$ Ω cm were used as substrates. By thermal oxidation a silicon oxide layer of about $d = 147 \pm 5$ nm was produced. Single-side-polished wafers were cut into rectangular pieces (10 \times 25 mm). Prior to the experiments, the wafers were cleaned with acetone and methanol and immersed into a solution of 1:1:5 (v/v) H_2O_2 (30%)/ NH_4OH (30%)/ H_2O for 5 min under ultrasonication.³⁸ The wafers were soaked for another 30 min at 60 °C, then they were rinsed intensively with water (Millipore, Molsheim, France; $R > 18$ $\text{M}\Omega$ cm^{-1} , $\text{pH} = 5.5$). The cleaned wafers were sonicated in a mixture of 1:1:6 (v/v) H_2O_2 (30%)/ HCl (37%)/ H_2O at 80 °C for 15 min and rinsed intensively with water. After these surface pretreatments, the contact angle of the wafer surface with water was almost zero.

Polymer Grafting Reaction. The silane-functionalized poly(2-oxazolines) were grafted onto the surface as previously reported.²⁰ The cleaned substrates were transferred from pure water into acetonitrile by stepwise exchange of the solvents. Then the wafer was immersed into a solution of 30 mg of the polymer dissolved in 10 mL of anhydrous acetonitrile under N_2 atmosphere, sonicated at 80 °C for 2 h. The grafting of the polymers was carried out under ultrasonication to prevent undesired physisorption and polymerization prior to the surface coupling.³⁹ After the coupling reaction, the sample was sonicated twice in fresh acetonitrile and rinsed intensively in order to remove physisorbed material from the surface. Each polymer-coated sample was dried at 70 °C and stored in a closed box separately.

Static Swelling Measurements. The equilibrium film thickness of the grafted film was measured at room temperature (293 K) by a conventional PCSA (Polarizer-Compensator-Sample-Analyzer) ellipsometer (Plasmos GmbH Prozesstechnik, München,

(37) Persigehl, P.; Jordan, R.; Nuyken, O. *Macromolecules* **2000**, *33*, 6977.

(38) Kern, W.; Puotinen, D. A. *RCA Rev.* **1970**, *31*, 187.

(39) Here, control experiments were performed to verify that the ultrasonic treatment did not effect the degree of polymerization. In short: PEOX30 was irradiated for several hours by the same ultrasonic source and analyzed by matrix-assisted laser desorption ionization time-of-flight mass spectrometry and GPC. No significant changes could be detected either in the mass spectra or in the GPC elution curves.

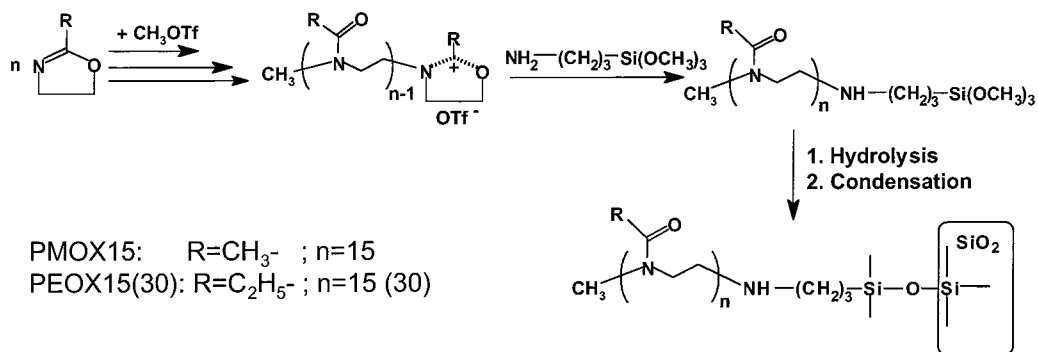


Figure 1. Synthesis of silane end functionalized poly(2-alkyl-2-oxazoline)s and consecutive grafting reaction onto silicon dioxide surfaces.

Germany) at a constant wavelength ($\lambda = 632.8$ nm) and a fixed angle of incidence (70°). Total Fresnel reflection coefficients R_p and R_s are related⁴⁰ to two ellipsometric angles Δ and Ψ

$$R_p/R_s = \tan \Psi \exp(-i\Delta) \quad (1)$$

Absolute values of the thickness and the refractive index can be estimated from the measured Δ and Ψ computer-assisted analysis. The complex refractive indices were assumed, $n = 3.868 - j0.024$ for bulk silicon⁴¹ and $n = 1.46$ for silicon dioxide,⁴² respectively.

The initial thickness of the monolayer (i.e., thickness under low humidity conditions) was determined at a relative humidity of around 4%, by assuming the refractive index of the dry film, $n_0 = 1.52$.⁴³ To take statistical values for the background data and the initial film thickness, three points were measured for each sample. Relative humidity inside the measurement chamber was precisely controlled by a self-made humidity chamber.^{3,35,36} Between two subsequent equilibrium thickness measurements, the film was allowed to equilibrate for about 10 min. The refractive index of the swollen polymer film with increasing amount of water was adjusted by applying the Garnet equation^{44,45} that relates the refractive index n_F of a solution to the volume fraction Φ :

$$n_F = n_M \left(1 + \frac{3\Phi}{\left(\frac{n_0^2 + 2n_M^2}{n_0^2 - n_M^2} \right) - \Phi} \right)^{1/2} \quad (2)$$

n_0 and n_M are the refractive indices of the pure solute and the pure solvent, respectively. The volume fraction Φ is simply represented by the layer thickness d : $\Phi = d_0/d$, where d_0 is the initial film thickness. The equilibrium film thickness at certain humidity can be calculated self-consistently, starting from the refractive index of the initial layer and successively applying the Garnet formula.

It is noteworthy that in our experimental system there is no bulk water. Below the condensation limit, the film is swollen by water vapor. The sum of the operating forces within the film (i.e., disjoining pressure) is at the equilibrium with the osmotic pressure of the atmosphere in the climate chamber. This external pressure, p , can be defined as the negative derivative of Gibbs free energy G , with respect to the film thickness d , $p = -\partial G/\partial d$. G is the free energy of the film, which is a function of the thickness d and the water volume fraction within the film. The disjoining pressure can be expressed by use of van't Hoff's law^{46,47}

$$p = -\left(\frac{RT}{V_m} \right) \ln \left(\frac{p_w}{p_0} \right) = -\left(\frac{RT}{V_m} \right) \ln(X) \quad (3)$$

where V_m is the molar volume of water and T is the temperature. R stands for the gas constant, and X is the relative humidity inside the chamber, which is equal to the ratio between the actual vapor pressure p_w and the saturation pressure of water in the surrounding atmosphere p_0 .^{48,49} To analyze the force–distance relationship, the determined layer thickness was plotted versus

the relative humidity (i.e., disjoining pressure), yielding the disjoining pressure–thickness curve.^{36,50,51}

Dynamic Swelling Measurements. Prior to the dynamic swelling experiments, the sample was kept in the dry atmosphere (relative humidity $\sim 4\%$) for at least 15 min. With our standard ellipsometry setup, a single data point is available every 1.7 s. After 50 data points were measured (i.e., 85 s), the flow of dry air was switched to that of the highly humid air (relative humidity $\sim 90\%$). After 1000 measurements, the flow was switched back to the dry one and another 1000 data points were recorded. Changes in the absolute film thickness were plotted as a function of time to investigate the kinetics of the swelling of the polymers under “osmotic shocks”.

Results and Discussion

Silane-functionalized poly(2-alkyl-2-oxazoline)s were synthesized by the living cationic polymerization of 2-alkyl-2-oxazolines, followed by termination with a nucleophile trimethoxysilane groups (see Figure 1). Different from the previous report,¹⁹ methyl triflate was used as the initiator for a fast initiation and a propagation reaction via ionic species. (3-Aminopropyl)trimethoxysilane was chosen for the termination because of the higher reactivity of the methoxysilane group to silicon dioxide surfaces. The successful termination and functionalization reaction was confirmed by ¹H NMR and FTIR spectroscopy. Since the signals of the (aminopropyl)trimethoxysilane moiety are superimposed by signals of the polymer, a characteristic signal at δ 0.5 of the $-CH_2-Si(OCH_3)_3$ methylene group appears in all spectra. In the FTIR spectra the presence of the methoxysilane moieties was verified by the appearance of characteristic vibrational bands at 1031 and 1061 cm^{-1} .⁵² As summarized in Table 1, high yields and narrow polydispersities between 1.06 and 1.17 denote the highly living ionic polymerization and effective termination. In all cases, the chain length

(40) Azzam, R. M. A.; Bashara, N. M. *Ellipsometry and Polarized Light*; North-Holland: Amsterdam, 1977.

(41) Tompkins, H. G. *User's Guide to Ellipsometry*; Academic Press: San Diego, CA, 1993.

(42) Jellison, G. E. *J. Appl. Phys.* **1991**, *69*, 7627.

(43) Tomalia, D. A.; Killat, G. R. *Encyclopedia of Polymer Science and Engineering*; Wiley: New York, 1985.

(44) Garnet, M. *Philos. Trans. A* **1904**, *203*, 385.

(45) Garnet, M. *Philos. Trans. A* **1906**, *205*, 237.

(46) Landau, L. D.; Lifschitz, E. M. *Lehrbuch der theoretischen Physik, Band V, Statistische Physik*; Akademie-Verlag: Berlin, 1987.

(47) Israelachvili, J. N. *Intermolecular and Surface Forces*, 2nd ed.; Academic Press: London, 1992.

(48) Rand, R. P. *Annu. Rev. Biophys. Bioeng.* **1981**, *10*, 277.

(49) Rand, R. P.; Parsegian, V. A. *Biochim. Biophys. Acta* **1989**, *351*.

(50) Parsegian, V. A.; Fuller, N.; Rand, P. *Proc. Natl. Acad. Sci. U.S.A.* **1979**, *76*, 2750.

(51) Pashley, R. M.; Kitchener, J. A. *J. Colloid Interface Sci.* **1979**, *71*, 491.

(52) Bellamy, L. J. *The Infrared Spectra of Complex Molecules*; Chapman and Hall: London, 1975.

Table 1. Data of Synthesized PMOX and PEOX

polymer	[M] ₀ /[I] ₀ ^a	yield (%) ^b	M _n (GPC) ^c	M _w (GPC) ^d	PDI ^e	DP _{NMR} ^f
PMOX15	15	98	1712	1849	1.08	16
PEOX15	15	71	1525	1622	1.06	17.5
PEOX30	30	87	2408	2824	1.17	30

^a Initial monomer/initiator feed. ^b Yield calculated against initiator. ^c M_n, number average as determined from gel permeation chromatography (GPC) trace. ^d M_w, weight average from GPC trace. ^e M_w/M_n, polydispersity index (PDI). ^f Degree of polymerization (DP) calculated from ¹H NMR spectra (end group analysis).

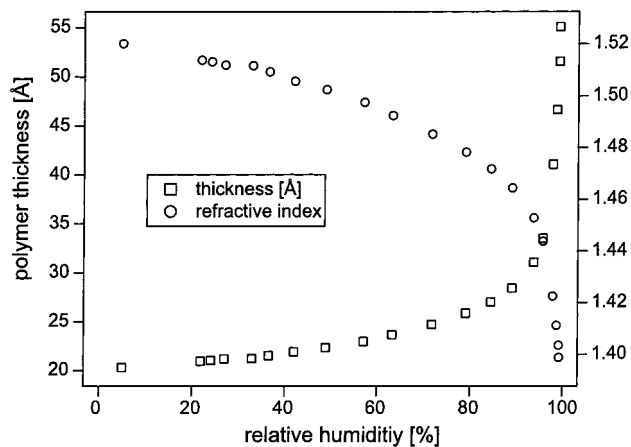


Figure 2. Equilibrium thickness (left ordinate) and refractive indices derived from the Garnett equation (right ordinate) of a grafted PMOX15 film plotted versus relative humidity of the atmosphere. Significant changes in the film thickness were observed under relative humidity conditions >90%.

could be obtained by signals in the ¹H NMR spectra from the endgroups. However, all values of M_n and M_w determined by GPC seemed to be too low, which might be due to the calibration with polystyrene standards.^{20,22,37}

The homogeneity of the surface coating was checked by scanning probe microscopy.⁵³ The root mean square roughness of a freshly cleaned silicon/silicon dioxide substrate was ~0.2 nm within a 1 × 1 μm² area. The surfaces coated with PMOX15 and PEOX15 showed a slight increase in root mean square roughness to ~0.4 nm, while the grafting of the longer polymer PEOX30 resulted in root mean square values of ~0.6 nm.

Static Swelling Behavior. In Figure 2, changes in the equilibrium thickness of a grafted PMOX15 brush with an initial dry thickness of d₀ = 20 Å are plotted versus relative humidity of the atmosphere. Thickness deviations among the three different measurements over this sample were within the range of ±2 Å, denoting a homogeneous grafting of the polymer chains onto the silicon wafer over the entire substrate. Refractive index and thickness of the swollen PMOX15 brush (i.e., PMOX15–H₂O mixture) were calculated self-consistently with the Garnett equation (eq 2) and plotted as a function of relative humidity (Figure 2). The thickness at the highest humidity condition (~98%) d_{max} yielded the maximum swelling ratio, ρ_{max}(PMOX15) = d_{max}/d₀ = 2.7. It should be noted that measurements of the maximum film thickness d_{max} include experimental errors, arising from the hygrometer near the condensation limit as well as from the significant changes in the film thickness under highly humid atmospheres (relative humidity >90%).

(53) Scanning probe microscopy studies were obtained in tapping mode with a Nanoscope IIIa, Multimode from Digital Instruments. Each polymer brush was examined at least at three different locations within areas of 100 × 100 and 1 × 1 μm².

Table 2. Initial Dry Thickness, d₀, and Maximum Swelling Ratio, ρ_{max}, of the Grafted Poly(2-oxazoline) Films Measured by Ellipsometry

polymer	d ₀ ^a (Å)	ρ _{max}
PMOX15	18.2–21.7	2.7–3.4
PEOX15	12.4–20.8	2.8–3.5
PEOX30	24.4–39.7	1.6–1.8

^a d₀ was determined at a relative humidity of ~4%, by assuming the refractive index n₀ = 1.52.

In Table 2, d₀ and ρ_{max} obtained for all three types of polymers are summarized for the different substrate modifications. As shown in the table, d₀ values exhibited certain deviations among different samples, especially for the films of PEOX15 (d₀(PEOX15) = 12.4–20.8 Å) and PEOX30 (d₀(PEOX30) = 24.4–39.7 Å).⁵⁴ These might be attributed to the grafting of the polymers “onto” the substrate from the solutions. However, the variations of the maximum swelling ratio ρ_{max} are rather small, reflecting the characteristic water uptake ability of each polymer. Despite the different side chains, PMOX15 films had comparable d₀ values (d₀(PMOX15) = 18.2–21.7 Å) to PEOX15 films. The similar d₀ values indicate that the grafting densities of these two polymers are similar. ρ_{max} values showed even smaller error bars, ρ_{max}(PMOX15) = 2.7–3.4 and ρ_{max}(PEOX15) = 2.8–3.5, respectively. The initial thickness (d₀(PEOX30)) of the PEOX30 was larger than d₀(PEOX15), which is plausible from its longer chain length. On the contrary, ρ_{max} of the PEOX30 brush, ρ_{max}(PEOX30) = 1.6–1.8, was obviously smaller than the corresponding values obtained for the films of PMOX15 and PEOX15. These observations suggested that the static swelling behaviors of the poly(2-oxazoline) films are dependent not on the side chains but on the chain length.

The equilibrium hydration mechanisms were quantitatively analyzed by the force–distance curves, i.e., the disjoining pressure–film thickness relationships. In Figure 3, the disjoining pressure calculated from eq 3 is plotted as a function of film thickness for the PMOX15 film, the same film as shown in Figure 2.

At the high disjoining pressure conditions, P > 1 × 10⁷ Pa, the film is compressed and strong repulsive forces operate due to the overlapping of orbitals. In this regime, the strong repulsive forces can be described by a power-law potential:⁴⁷

$$P(\rho) \sim \rho^{-n} \quad (4)$$

where n is an integer between 9 and 16. In a logarithmic plots, this high-pressure regime can be separated into two distinct regimes: [i] between P = 5 × 10⁸ Pa and 2 × 10⁸ Pa with exponent n₁ > 20, and [ii] between P = 2 × 10⁸ Pa and 1 × 10⁷ Pa with exponent n₂ = 7.9. For these two repulsive regimes, the same fitting routines were applied to the other samples. The obtained results are given in Table 3. Since the thickness changes in the first regime are very small (approximately 1–2 Å), this regime

(54) The area per grafted chain A_{chain} was roughly estimated by using the bulk density of poly(ethylloxazoline), ρ = 1.14 (Chen et al. *Polymer* **1994**, *17*, 3587). From the dry thickness of 2 nm and M_w = 1500 (representative values for n = 15), we obtain A_{chain} = M_w/d₀r ~ 1.1 nm². The corresponding value for n = 30 (d₀ = 3 nm and M_w = 3000) is about 1.5 nm². These values are remarkably larger than the area per non-cross-linked trimethoxy headgroups, 0.45 nm² (Fontaine et al. *Langmuir* **1999**, *15*, 1348). Since the radius of gyration scales with N^{1/2}, we could approximate R_g from the previous light scattering study of Chen et al. (Chen et al. *Macromolecules* **1990**, *23*, 4688), yielding R_g ~ 1.7 nm for n = 15 and R_g ~ 2.5 nm for n = 30, respectively. Here, the distance between two grafting points calculated from the area per chain (1.2–1.4 nm) is smaller than 2R_g so that each chain interacts with the nearest neighbors.

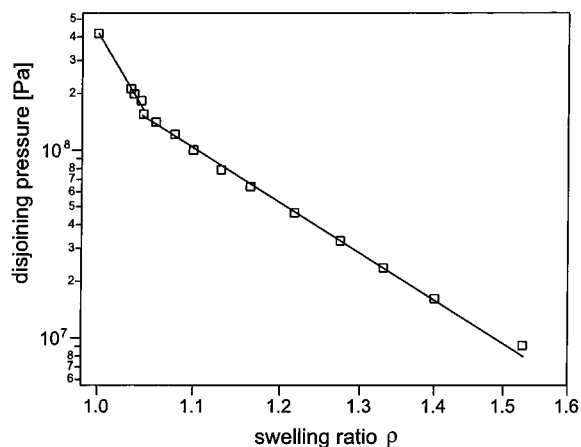


Figure 3. Disjoining pressure calculated from relative humidity plotted as a function of PMOX15 film thickness. In the double logarithmic plots, this regime under high pressure can be separated into two regimes: [i] between $P = 5 \times 10^8$ Pa and 2×10^8 Pa with exponent $n_1 > 20$ and [ii] between $P = 2 \times 10^8$ Pa and 1×10^7 Pa with exponent $n_2 = 7.9$.

Table 3. Exponents for the Power-Law Potential $P(\rho) \sim \rho^{-n}$ Calculated for Two High Disjoining Pressure Regimes: [i] n_1 for 5×10^8 to 2×10^8 Pa, and [ii] n_2 for 2×10^8 to 1×10^7 Pa

polymer	n_1	n_2
PMOX15	18–24	6.6–8.5
PEOX15	12–34	6.5–8.4
PEOX30	32–33	12

with very high exponents ($n_1 = 34$ – 12) is close to a theta function ($n = \infty$), reflecting the incompressibility of the chains. On the other hand, the exponents in the second regime are smaller. The exponent n_2 calculated for the shorter polymers (PMOX15 and PEOX15) stays in the same range, $n_2 = 6.5$ – 8.5 . In contrast, n_2 of PEOX30 films was obviously larger, $n_2 = 12$. As the repulsive forces become weaker according to the finite compressibility of the films in this second regime, it is possible that additional contributions such as entropic polymer interaction and/or conformational changes of the chains become observable.

The third regime, at $P < 1 \times 10^7$ Pa, is dominated by the hydration of polymer layer. As the experiments were carried out under humidity conditions below the condensation limit, there is no bulk water around the polymer chains. Here, the osmotic pressure within the film (i.e., disjoining pressure) is too high to treat the grafted chains as “mushrooms” or “stretched brushes” according to the conventional theorem.^{55–59} Thus, we introduce an empirical fit^{48,49} to interpret the hydration forces between two hydrophilic surfaces, following an exponential decay

$$P_h = P_0 \exp(-D/\lambda_h) \quad (5a)$$

$$P_h = P_0 \exp(-\rho/\lambda^*) \quad (5b)$$

with λ_h as the decay length. D denotes the separation between surfaces, and P_0 is an intrinsic pressure.⁶⁰ To compare the hydration of polymers with different initial thickness, the disjoining pressure was plotted as a function

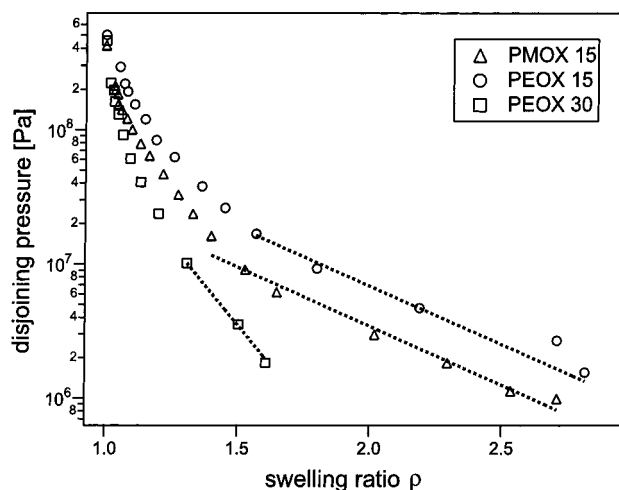


Figure 4. Force–distance relationship in single logarithmic plots for the third regime, [iii] at $P < 1 \times 10^7$ Pa. To compare the hydration of polymers with different initial thickness, the distance was given by the swelling ratio. Hydration forces exponentially decay according to $P_h = P_0 \exp(-\rho/\lambda^*)$, where λ^* is the decay constant and P_0 an intrinsic pressure.

Table 4. Intrinsic Pressure, P_0 , and Decay Constant, λ^* , Calculated in the Lower Disjoining Pressure Regime, $P < 1 \times 10^7$ Pa

polymer	P_0 (Pa)	λ^*
PMOX15	1.8×10^8 to 2.0×10^8	0.49–0.56
PEOX15	1.6×10^8 to 1.8×10^8	0.48–0.63
PEOX30	1.4×10^{10} to 4.5×10^{10}	0.16–0.18

of the swelling ratio ρ in a semilogarithmic plot (Figure 4). In the same manner, the decay constant $\lambda^* = \lambda_h/d_0$ was normalized. For the fitting procedure, the errors from humidity measurements were kept below $\pm 1.5\%$. As summarized in Table 4, the obtained decay constant λ^* showed a clear dependence on the chain length. The calculated λ^* values for the shorter polymers, PMOX15 and PEOX15, are in good agreement ($\lambda^* = 0.5$ – 0.6). Compared to these values, λ^* obtained for PEOX30 brushes was significantly smaller by a factor of 2–3 ($\lambda^* = 0.2$). Moreover, the intrinsic pressure P_0 for PEOX30 films was about 2 orders of magnitude larger, $P_0 > 10^{10}$ Pa, associated with lower λ^* values.

Previously, Lehmann and R ue had reported the grafting of poly(ethyloxazoline) with disulfide groups onto gold surfaces.²¹ Compared to our results, the reported initial thickness values $d_0 = 3.0$ – 3.5 nm for the polymers with more than 50 monomer units are small, especially considering the long alkyl ($-C_{11}H_{22}-$) spacers between the disulfide group and the polymer backbone. They had also measured the swelling behaviors by surface plasmon resonance (SPR) under relative humidity conditions controlled by different salt solutions. However, only two or three data points had been given at the humidity conditions above 80%, with the estimated maximum swelling ratio, $\rho_{\max}(\text{PEOX150}) = 1.4$. These results might be attributed to the poorer grafting density, which is reasonable from the grafting of long polymers “onto” the substrates from the solution.

Dynamic Swelling Behavior. To obtain the characteristic time constants for the exchange of the atmosphere, the change of the relative humidity under osmotic shocks was monitored as a function of time. Different from an

(55) De Gennes, P. G. *J. Phys. (Paris)* **1976**, *37*, 1445.

(56) Alexander, S. *J. Phys. II* **1977**, *38*, 983.

(57) De Gennes, P. G. *Macromolecules* **1980**, *13*, 1069.

(58) Milner, S. T.; Witten, T. A.; Cates, M. E. *Macromolecules* **1988**, *21*, 2610.

(59) Milner, S. T.; Witten, T. A.; Cates, M. E. *Europhys. Lett.* **1988**, *5*, 413.

(60) It should be noted this treatment is originally for symmetrical systems so that the treatment of our “half system” should be multiplied by a factor of order of unity.

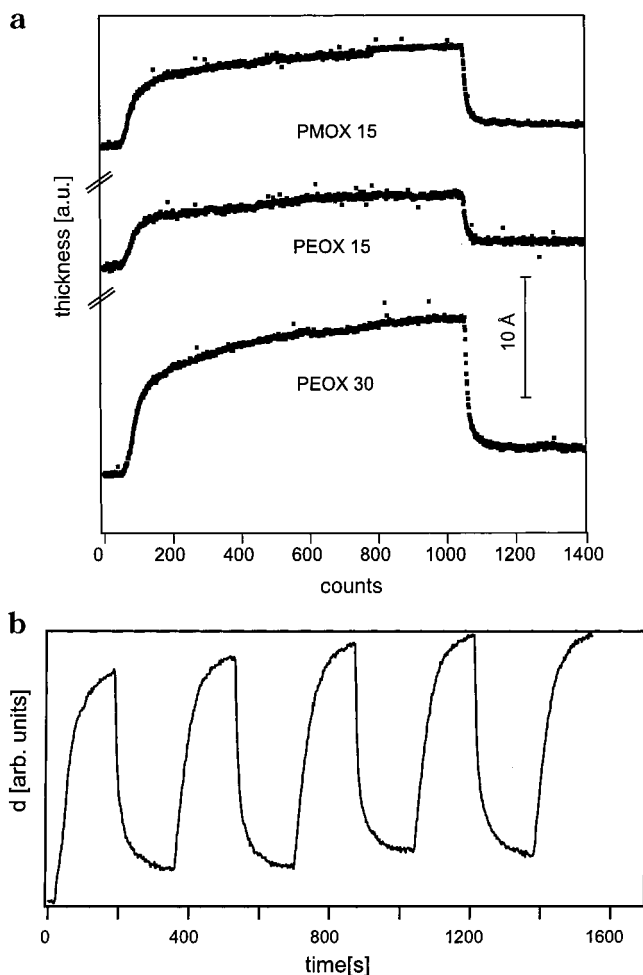


Figure 5. (a) Dynamic swelling curves of PEOX30 (top) and PEOX15 (bottom) films. Thickness changes are plotted as a function of time to study the kinetics of the swelling under "osmotic shocks". Prior to the dynamic measurements, the film was dried for 3 h at 70 °C and equilibrated with a dry atmosphere (humidity ~4%) for more than 15 min. A single count corresponds to 1.7 s. After the flow of dry air was switched to that of humid air (humidity ~90%), an increase of the film thickness could be observed. The characteristic time constants of the dynamic swelling curves were evaluated semiquantitatively by the time required to reach $d/d_{\max} = (1 - e^{-1}) \approx 0.63$. (b) Dynamic swelling curves of a PEOX15 film under several cycles of "osmotic shocks". The film thickness (in arbitrary units) is plotted as a function of time. A clear increase in the "dry" film thickness ($\Delta d_0 = 2-3 \text{ \AA}$) was observed when the humidity condition was switched back to 4%, which could be recovered by drying the sample at 70 °C for 3 h.

ideal osmotic pulse, the increase and decrease in the relative humidity can be approximated by a single exponential. The characteristic time constants were calculated to be $\tau = 35 \text{ s}$. Such delays might be due to (i) the distance between the switching valve and the chamber, (ii) the certainly large chamber volume (2 L) compared to the air flow rate (5 L/min), and (iii) the time resolution of the humidity sensor. Therefore, it is not possible to follow the fast hydration processes with smaller characteristic time constants using this experimental setup.

In Figure 5a, the dynamic swelling curves of PEOX15 and PEOX30 are presented, by plotting the thickness changes as a function of time. Prior to the dynamic measurements, the film was dried for 3 h at 70 °C and equilibrated with a dry atmosphere (4% relative humidity) for more than 15 min.

After the flow of dry air was switched to humid air (relative humidity ~90%), an increase of the film thickness

was observed. When the humidity condition was switched back to dry atmospheric conditions (Figure 5b), a clear increase in the "dry" film thickness ($\Delta d_0 = 2-3 \text{ \AA}$) was observed. This can be explained by an irreversible water uptake in the hygroscopic polymer brush layer. This apparent thickness increase could only be reversed by heating the sample to 70 °C for more 3 h under vacuum. Because of this clear hysteresis in the thickness recovery, the measured thickness changes under an "osmotic shock" could not be analyzed with simple exponential kinetics. Thus, the characteristic time constants of the dynamic swelling curves were evaluated semiquantitatively by the time required to reach $d/d_{\max} = (1 - e^{-1}) \approx 0.63$, where d_{\max} is the maximum thickness. Similar to the results of the static swelling experiments, the kinetics of the water uptake of the poly(oxazoline) brushes seemed to depend on the chain length of the polymer but not on the side groups. The characteristic time constant for the dynamic swelling of PEOX30, $\tau_{\text{PEOX30}} = 200 \text{ s}$, is obviously larger than those obtained for the shorter PEOX15 and PMOX15, $\tau = 140-150 \text{ s}$. Even though a quantitative analysis of the time constants is still difficult, the apparently slower swelling of PEOX30 is in accordance with the smaller swelling ratios obtained in the static swelling experiments. On the other hand, the characteristic time constant for the thickness decrease under an inverse "osmotic shock" ($\tau \sim 50 \text{ s}$) was comparable to that for the exchange of relative humidity; therefore, the kinetics of this fast process could not be resolved.

Conclusions

Poly(2-alkyl-2-oxazoline)s (PMOX15, PEOX15, and PEOX30) were synthesized by living cationic ring-opening polymerization and grafted onto silicon/silicon dioxide substrates. The presented synthetic pathway results in linear hydrophilic polymers of low polydispersities and quantitative end functionalization of the chains for surface grafting reactions.

Static swelling behavior of the grafted polymer films was studied by quantitative measurements of the equilibrium film thickness under precisely controlled relative humidity conditions. The maximum swelling ratios ρ_{\max} of the shorter polymer chains are comparable ($\rho_{\max} = 2.7-3.5$) despite their differences in the side chains, while ρ_{\max} of the PEOX30 film, $\rho_{\max(\text{PEOX30})} = 1.6-1.8$, was obviously smaller than the corresponding values obtained for the films of PMOX15 and PEOX15.

At high disjoining pressure conditions ($P > 1 \times 10^7 \text{ Pa}$), we observed two regimes where strong repulsive forces obey a power law, $P(\rho) \sim \rho^{-n}$: the first regime with large exponents ($n_1 = 34-12$) can be almost explained by a theta function, while the exponents in the second regime were apparently smaller. On the other hand, the third regime, $P < 1 \times 10^7 \text{ Pa}$, is dominated by hydration forces, which can be described by $P_h = P_0 \exp(-\rho/\lambda^*)$. Hydration of polymers with different initial thickness was compared by the normalized swelling ratio ρ . The decay constant λ^* also exhibited a clear dependence upon the chain length: $\lambda^* = 0.5-0.6$ for PMOX15 and PEOX15, and $\lambda^* = 0.2$ for PEOX30, respectively. These observations suggested that the static swelling behaviors of the poly(2-oxazoline) films are dependent not on the side chains but on the chain length.

Semiquantitative analysis of the dynamic swelling behavior of the poly(2-oxazoline) brushes suggested that the hydration kinetics also seemed to be dependent on the chain length but are not affected by the side chains. The characteristic time constant for PEOX30 films (τ_{PEOX30}

= 200 s) is larger than those for the shorter PEOX15 and PMOX15 ($\tau = 140\text{--}150$ s). To describe the kinetics more quantitatively, further technical improvement (e.g., fast exchange of the atmosphere, monitoring of humidity in the higher time resolution) will be required.

Since poly(2-oxazoline) used in this study can be terminally functionalized with alkyl chains,²⁰ this system is also a promising candidate for the fabrication of "tethered" lipid bilayers with polymer spacers.^{61–63} The chemical and morphological modification (e.g., control of hydrophilic/hydrophobic balance, grafting density, and chain length) allows precise control of interfacial properties

(61) Häussling, L.; Knoll, W.; Ringsdorf, H.; F. J., S.; Yang, J. *Macromol. Chem. Macromol. Symp.* **1991**, *46*, 145.

(62) Raguse, B.; Braach-Maksyvytis; Cornell, B. A.; King, L. G.; Osman, P. D. J.; Pace, R. J.; Wieczorek, L. *Langmuir* **1998**, *14*, 648.

(63) Wagner, M. L.; Tamm, L. K. *Biophys. J.* **2000**, *79*, 1400.

of the resulting brushes for the design of soft and functional bridges between semiconductor surfaces and biomaterials.

Acknowledgment. The authors are indebted to Professor E. Sackmann and Professor O. Nuyken for the constant support and helpful suggestions. This work was supported by the Deutsche Forschungsgemeinschaft (SFB 563 B7, Sa 246/27-2) and by the Fonds der Chemischen Industrie. M.T. is grateful to Alexander von Humboldt foundation for the postdoctoral fellowship and to DFG for the habilitation fellowship (Emmy Noether Programm). L.P. is thankful to the DAAD for a SOKRATES stipend. R.J. also acknowledges the stipend from the Dr. Hermann-Schnell-Stiftung of the GDCh.

LA0112559